Acoustic response of a feeding system to high-frequency transverse acoustic field

A. Ficuciello, F. Baillot, J. Blaisot, C. Richard, M. Theron

▶ To cite this version:

A. Ficuciello, F. Baillot, J. Blaisot, C. Richard, M. Theron. Acoustic response of a feeding system to high-frequency transverse acoustic field. Thermoacoustic Instabilities in Gas Turbines and Rocket Engines : Industry meets Academia, May 2016, Munich, Germany. hal-02370173

HAL Id: hal-02370173

https://hal.archives-ouvertes.fr/hal-02370173

Submitted on 19 Nov 2019

HAL is a multi-disciplinary open access archive for the deposit and dissemination of scientific research documents, whether they are published or not. The documents may come from teaching and research institutions in France or abroad, or from public or private research centers.

L'archive ouverte pluridisciplinaire **HAL**, est destinée au dépôt et à la diffusion de documents scientifiques de niveau recherche, publiés ou non, émanant des établissements d'enseignement et de recherche français ou étrangers, des laboratoires publics ou privés.

Acoustic response of a feeding system to high-frequency transverse acoustic field

A. Ficuciello[1] [3], F. Baillot[1], J.B. Blaisot[1], C. Richard[2] and M. Théron[3]

Abstract

The acoustic coupling between the injection system and the acoustic fluctuations in liquid rocket engine combustion chambers is an important issue in the understanding of the thermo-acoustic instability phenomenon. This paper presents results of a large parametric investigation of a two-phase injection system acoustic response, to the excitation produced by a high-amplitude transverse acoustic field forced into a main resonant cavity. Two domes, one for the gas and one for the liquid, were expressly designed to feed three identical coaxial injectors. Characterization of domes internal mode shapes were performed by measuring pressure signals at different locations in the domes. Experimental mode shapes showed good agreement with those predicted by numerical simulations. Acoustic pressure amplitudes up to 17% of the the one induced in the main cavity can be found in both gas and liquid dome. The maximum acoustic response is observed in a configuration in which acoustic boundary conditions does not correspond to the maximum injection system solicitation conditions.

Keywords

Acoustic coupling, Coaxial injector, Transverse mode, Liquid rocket engines

Introduction

The development of liquid rocket engine propulsion systems has historically been plagued by the phenomenon of combustion instabilities (see Yang and Anderson (1995) and Harrje and Reardon (1972)). Several programs were devoted to the investigation of this problem and both full-scale and sub-scale tests were performed (see, for example, Oefelein and Yang (1993), Fisher *et al.* (1995)). Hot fire tests indicate that, among the different types of combustion instabilities, high-frequency transverse instabilities are considered as the most harmful for liquid rocket engines operations.

Although many years of research have been dedicated to solving the problem there is still a lack of knowledge. The main problem comes from the numerous involved processes and sub-processes as well as from the complexity of their potential interactions. Combustion in liquid rocket engines is never perfectly steady and fluctuations of pressure, temperature and velocity are always present. Because the sub-processes that occur in between the injection and chemical reactions are dependent on the combustion chamber pressure and aerodynamics, a feedback mechanism able to amplify combustion chamber natural acoustic modes is often encountered (Hutt and Rocker

(1995)). The feedback mechanisms are commonly sub-classified into intrinsic and injection-coupled mechanisms. The intrinsic mechanism implies that only the processes taking place after propellant injection, are responsible for the chamber pressure fluctuation amplification. In the injection-coupled mechanism the acoustic fluctuations in the combustion chamber interact with the natural frequencies of the feeding system, causing flow rate fluctuations which give a significant contribution to the acoustic pressure amplification. It is thus clear that the feeding system design, in particular that of the injector elements, represents a key element for the stability of rocket engines.

This paper focuses on the interaction between the injection system and acoustic transverse fluctuations present in the chamber. The injection system is composed of three coaxial

[1]CORIA, UMR 6614, CNRS Université et INSA de ROUEN, BP 12, 76801 Saint Etienne du Rouvray, France
[2]LMRS, UMR 6085, CNRS-Université de ROUEN, BP 12, 76801 Saint Etienne du Rouvray, France
[3]CNES Launchers Directorate, 52 Rue Jacques Hillairet, 75612 PARIS Cedex, France

Corresponding author:
Antonio Ficuciello, CORIA, UMR 6614 - CNES Launchers Directorate, France.

Email: ficuciea@coria.fr

injectors and of two feeding domes, one for the gas and one for the liquid. The acoustic field is forced in a semi-open resonant cavity by 4 compression drivers. A parametric investigation is performed in order to characterize the sensitivity of the injection system to some of its key geometrical features.

It will be shown that the injection system response is strongly affected by the position of the injectors along the acoustic axis, by the size of the domes and by the dimensions of the connections between domes and injectors. A part of the experimental results is compared with numerical simulations performed with COMSOL Multiphysics® Software. The software was also used in the design process of the two injection domes. Some key aspects of the design procedure is discussed hereafter.

Experimental set-up

The experimental set-up is composed of an acoustic semi-open resonant cavity with two parallel and vertical steel plates, and a roof and floor made of PVC. A pair of compression drivers Beyma CP850Nd is placed on each vertical plate to excite the 2nd transverse mode of the cavity. In the reference frame $\vec{x}$ is the horizontal direction parallel to the cavity walls; $\vec{y}$ the direction perpendicular to the walls and aligned with the acoustic axis, a.a.; $\vec{z}$ is the vertical descending direction. Acoustic pressure up to 174 dB can be reached in the cavity at a frequency of 1 kHz.

This experimental set-up was previously used to characterize the influence of the acoustic field on the atomization process by using 1 to 3 identical coaxial liquid/gas injectors, fed by independent lines (see Baillot *et al.* (2009) and Ficuciello *et al.* (2015)). Water and air were used as working fluids.

Here, the injection system has been modified by implementing two feeding domes, in order to link the three injectors. The entire system is conceived in a way that a large number of design parameters can be modified to investigate their influence on the acoustic coupling. In addition to them, the injection conditions and the position of the injection system along the acoustic axis, are also considered. Domes' parameters will be discussed below. Pressure signals are recorded at different locations in the main cavity and in the two injection domes. The entire set-up is placed in an acoustically isolated room.

A LabVIEW interface and a NI cDAQ module are used to manage the experiments. A dedicated software has been developed to automate the generation and the acquisition of
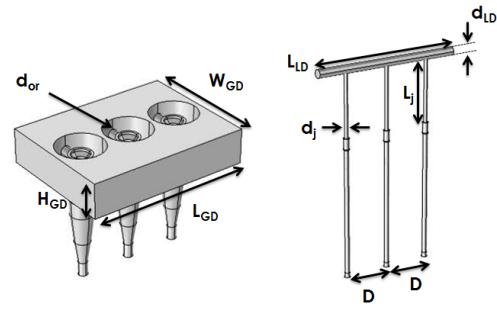

Figure 1. Gas dome GD (left side) and liquid dome LD (right side) internal domains considered in the numerical simulations.

the acoustic signals and to synchronize images acquisition when they are needed.

Domes' characteristics

The design of the two injection domes has been performed by taking into account the geometry of the three injector bodies that were already available. This fixed some constrains in terms of dome geometry. A numerical parametric analysis has been performed with the acoustic module COMSOL Multiphysics® in order to determine the best configurations. Figure 1 shows the final internal domes domains considered in the simulations. The shape and the size of each dome have been selected in order to have eigenfrequencies, $f_{m,n,p}$ close to the frequency of the acoustic field forced in the main cavity, e.g. 1 kHz. Here m, n and p indicate the number of nodes respectively in the direction x, y and z.

The ***gas dome GD*** (left side in Figure 1) presents a rectangular section and encloses a part of the three injector bodies. The link between an injector and the dome is ensured by two diametrically opposite holes drilled in the injector body. The diameter of these holes d_{or} can be changed by replacing the internal insert. The length L_{GD} and the height H_{GD} of the dome have been fixed as simulations indicated that the width W_{GD} of the dome was the parameter that mostly affected the resonant modes of interest. Thus, two pistons have been placed on the vertical boundary surfaces in order to vary the dome size W_{GD}. The smallest gas dome volume will be indicated in the following as $GD0$ and the biggest one as $GD8$.

The mode shapes of the three GD eigenfrequencies closer to 1 kHz, as predicted by the simulations, are represented in Figure 2. Characterization of numerical mode shapes is given as function of reduced coordinates: $\tilde{x}_g = x/W_{GD}^{max}$, $\tilde{y}_g = y/L_{GD}$ and $\tilde{z}_g = z/H_{GD}$. The numerical acoustic pressure distributions along $\tilde{x}_g$ and $\tilde{y}_g$ are also reported in Figure 2.
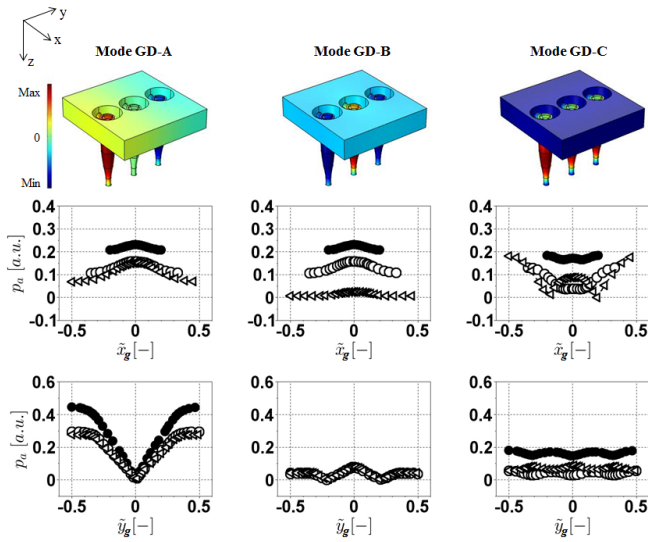
Figure 2. Gas dome mode-shapes obtained with COMSOL Multiphysics® and absolute acoustic pressure distribution w.r.t. $\tilde{x}_g = x/GD8$ and $\tilde{y}_g = y/L_{GD}$ for • $GD0$; ○ $GD4$ and ◁ $GD8$ ($d_{or} = 1.125$).
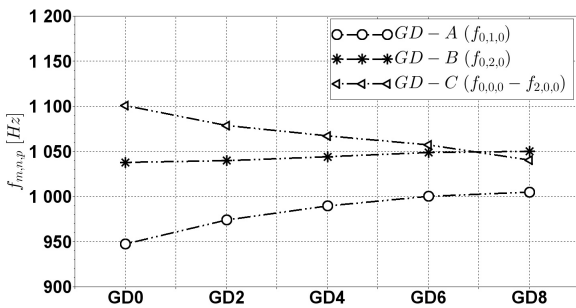

Figure 3. Gas dome eigenfrequencies as function of dome size ($d_{or} = 1.125$).

The influence of the dome size on the mode frequencies is indicated in Figure 3.

Calculations indicate that eigenfrequency associated with mode GD-A increases from 950 to 1005 Hz by increasing the dome size. Numerical acoustic pressure distributions indicate that all points are in-phase in any vertical planes $\tilde{x}_g\tilde{z}_g$ and that acoustic pressure amplitudes are slightly arched ($\tilde{z}_g = z/H_{GD}$). The vertical symmetry plane $\tilde{y} = 0$ is the nodal plane ($f_{0,1,0}$). Increasing the dome size decreases acoustic pressure amplitudes.

Mode GD-B presents a spatial structure similar to GD-A along the $\tilde{x}_g$ axis. In the horizontal plane $\tilde{x}_g\tilde{y}_g$ two nodal lines parallel to $\tilde{x}_g$ are identified, $f_{0,2,0}$. Increasing the dome size leads to a quasi-constant associated eigenfrequency, ranging between 1040 and 1050 Hz while the acoustic pressure amplitude decreases.

The third mode, named GD-C changes its shape as the dome size is increased. For dome sizes smaller than $GD6$, all points in the dome cavity are in phase and the dome acts as an Helmholtz resonator ($f_{0,0,0}$). For dome sizes larger than $GD6$ two nodal lines appear in the direction parallel to $\tilde{y}_g$ ($f_{2,0,0}$). In the $\tilde{x}_g$ direction, acoustic pressure amplitudes measured at the dome extremities, are of the same order of magnitude of those observed for $GD0$. Increasing the dome size produces an associated eigenfrequency which decreases from 1100 Hz to roughly 1040 Hz.

The ***liquid dome LD*** (right side in Figure 1) has a cylindrical geometry. The diameter of the dome d_{LD} is fixed in this analysis, while its length L_{LD} can be varied by means of two pistons. The smallest liquid dome volume is indicated in the following as $LD0$ while the biggest one as $LD2$. The dome is connected to the injectors by three connection junctions. The length L_j and the diameter d_j of the junctions are two adjustable parameters. In Figure 1, D indicates the distance between two successive injection axes.

Figure 4 represents two eigenmodes predicted by the simulations. Reduced coordinates considered for the liquid mode characterization are: $\tilde{x}_l = x/d_{LD}$, $\tilde{y}_l = y/L_{LD}$ and $\tilde{z}_l = z/d_{LD}$. Numerical along with the acoustic pressure distribution in the $\tilde{y}_l$ direction. Their corresponding eigenfrequencies are shown in Figure 5 as functions of the liquid dome size. The eigenfrequency associated to mode LD-A is around 1000 Hz for all dome sizes. If the eigenmode is excited all points are in-phase ($f_{0,0,0}$). Mode LD-B is reported here even if its corresponding eigenfrequency is around 3500 Hz, because its spatial structure indicates the presence of a pressure node at the central injector whilst the two domes extremities oscillate out-of-phase. Such a mode shape is used in the following to interpret experimental results.

The entire injection system assembly is shown in Figure 6 along with the main cavity. Three different configurations are shown:

- IPI - The central injector exit is placed at the pressure anti-node (PAN) where acoustic pressure level is maximum and the two lateral ones at two intensity anti-nodes (IAN). The three injectors' exits are submitted to in-phase cavity pressure fluctuations. The intensity anti-node is defined as the location where the product between the acoustic pressure and velocity fluctuations is maximum in the cavity;

- PIV - injectors' exits are submitted to different excitation conditions: velocity (VAN), intensity (IAN) and pressure anti-node (PAN) respectively;
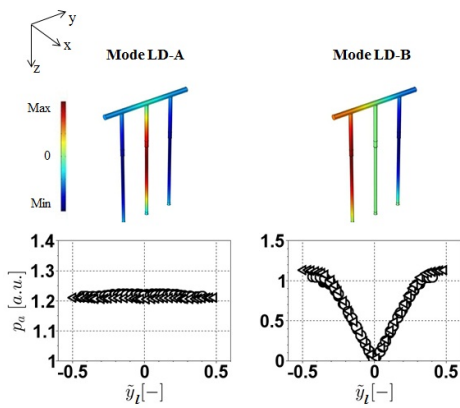
Figure 4. Gas dome mode-shapes obtained with COMSOL Multiphysics® and absolut acoustic pressure distribution w.r.t. $\tilde{y}_l = y/L_{GD}$ for ● $LD0$; ○ $LD1$ and ◁ $LD2$ ($L_j = 0.548$, $d_j = 0.67$).
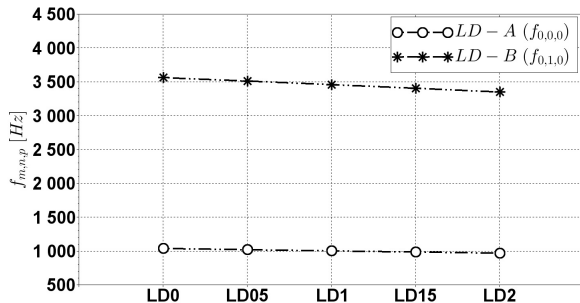

Figure 5. Liquid dome eigenfrequencies as function of dome size ($L_j = 0.548$, $d_j = 0.67$).

- IVI - The central injector exit is placed at the velocity anti-node (VAN) and the two lateral ones at two intensity anti-nodes (IAN), oscillating out-of-phase (non-symmetric excitation conditions).

The ability to change the size of the two domes, the kind of connections and the position of the injection system along the acoustic axis direction, provides a unique capacity of testing several resonant and coupling conditions with the same test bench.

Up to 4 pressure transducers (PCB 106B) can be placed on the gas dome at the same time in order to characterize its acoustic response (see Figure 7). The liquid dome is provided with two pressure transducers PCB 113B28, which are flush-mounted inside the pistons. A reference pressure is also measured in the main cavity at PAN.

Results and discussion

All tests have been performed by forcing the 2nd transverse cavity mode at a frequency of 1 kHz; the maximum available acoustic pressure level corresponds to an amplitude
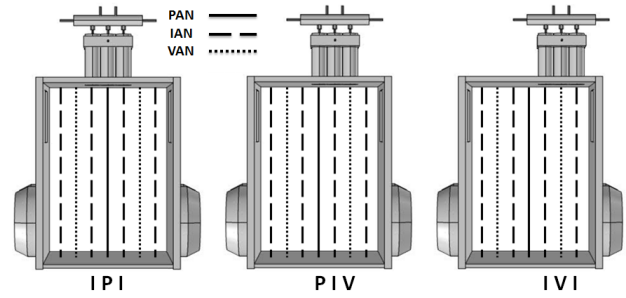

Figure 6. Scheme of the injection system placed on the main cavity roof according to three test configurations.
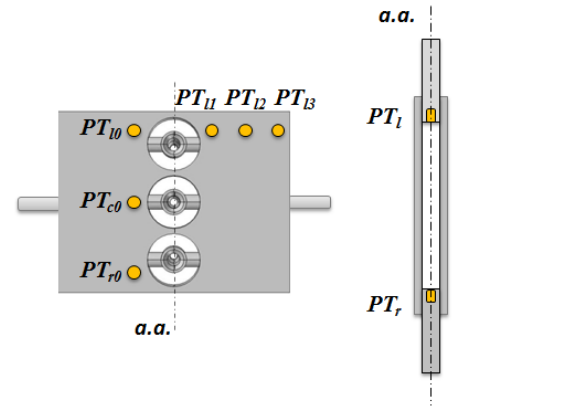

Figure 7. Schematic representation of pressure transducer locations in the gas dome (left side) and in the liquid dome (rigth side). Pressure transducers are represented in yellow.

of 12 kPa. Results indicate that both gas and liquid domes are sensitive to acoustic coupling; the maximum acoustic pressure fluctuation is 2000 Pa (160 dB), which corresponds to 17% of the acoustic pressure level in the main cavity at the pressure anti-node.

Acoustic response of the gas dome

A total of 180 test configurations were investigated to characterize the acoustic response of the gas dome , combining:

- five dome sizes indicated as: $GD0$, $GD2$, $GD4$, $GD6$ and $GD8$, with $GD0$ representing the smallest dome volume and $GD8$ the biggest one;
- three injector connection diameters (scaled with the outer injector exit diameter): $d_{or} = 0.375$, $d_{or} = 0.75$ and $d_{or} = 1.125$;
- four air mass flow rates (scaled with the biggest mass flow rate): $\tilde{m}_{air} = 0$, $\tilde{m}_{air} = 0.4$, $\tilde{m}_{air} = 0.7$ and $\tilde{m}_{air} = 1$;
- three spatial configurations of the injection system with respect to the acoustic axis (see Figure 6).

For all the considered configurations, results indicate that the injection system response is strongly affected by the acoustic boundary conditions at the injectors' outlets and by the design parameters. Figures 8 and 9 show the acoustic pressure amplitude measured with the pressure transducers inside the dome, while Figure 10 summarizes pressure transducers phase-shifts.

In all the configurations the acoustic level measured in the dome decreases roughly linearly with the dome size and with the mass flow rate. A decrease of the acoustic pressure amplitude is also observed by decreasing the orifice diameter d_{or}.

The IVI configuration manifests the strongest acoustic response. A maximum of 2800 Pa is measured without any flow rate. Increasing the mass flow rate decreases the dome acoustic response. For the maximum flow rate considered here ($\tilde{m}_{air} = 1$) the acoustic pressure fluctuation amplitude reaches 2000 Pa, namely 17% of the acoustic pressure fluctuation amplitude imposed in the main cavity at the pressure anti-node. The intensity of the acoustic response of the injection system attains a maximum of 1600 Pa and 800 Pa at PIV and IPI respectively.

Influence of d_{or} on the acoustic coupling between the main cavity and GD is also noticed in the phase-shift of the PT_{l0} signal with the signal of PT_{c0}, PT_{r0} or PT_{l1} as well as PT_{ref} signal from the transducer placed in the main cavity at PAN. For the IVI configuration with $d_{or} = 0.75$ the phase-shifts are independent of the dome size. With $d_{or} = 1.125$ acoustic coupling is facilitated and the phase-shift between PT_{l0} and PT_{ref} varies continuously with the dome size. Since the change in the dome size modifies the internal mode shapes, the phase-shift between two spatially fixed point is affected. On the contrary, in the presence of a small diameter ($d_{or} = 0.75$) boundary conditions near the orifice are not far from those given by a wall condition; thus, measurement at PT_{l0} does not vary with GD size. In this configuration (IVI) the mode shapes established in each cavity are independent and thus phase-shift between PT_{l0} and PT_{ref} is maintained fixed. Pressure fluctuations in the injection exit plane are out-of-phase at the two lateral injectors. This acoustic boundary conditions should excite the eigenmode GD-A of the gas dome revealed by the simulations; this is confirmed experimentally. The mode shape structure is well established: PT_{l0} and PT_{r0} are always out-of-phase while PT_{l0} and PT_{l1} are in-phase whatever the dome size. The three pressure transducers signals have the same acoustic pressure fluctuation amplitudes, which are always higher than the one of PT_{c0}. As observed for the phase-shift between the acoustic cavity and the gas dome, for
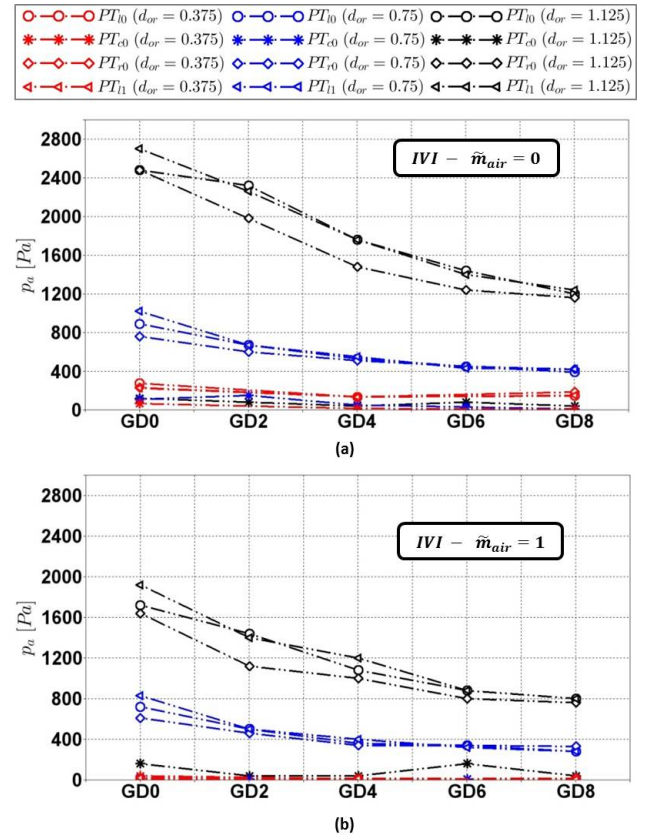

Figure 8. Acoustic response of the gas dome as a function of the dome size for the three connections diameters at: (a) IVI, $\tilde{m}_{air} = 0$ and (b) IVI, $\tilde{m}_{air} = 1$.

an orifice connection diameter of $d_{or} = 1.125$ the phase-shift inside the gas dome, i.e. between PT_{l0} and PT_{c0} varies between 45° and 90°, due to the modification of the dome internal mode shapes. For a smaller orifice diameter ($d_{or} = 0.75$) PT_{l0} and PT_{c0} are always in quadrature. Pressure transducers PT_{l2} and PT_{l3} provide complementary information on the acoustic pressure distribution inside the dome, giving the acoustic pressure amplitude in front of the piston for $GD4$ and $GD8$ respectively. Their acoustic pressure amplitudes are lower than PT_{l0} confirming that by increasing the dome size the acoustic pressure level decreases, which is in agreement with calculation relative to mode GD-A presented in Figure 2.

For the PIV configuration the dome is submitted to the larger pressure fluctuation range, due to the presence, at the injectors exit, of a pressure and a velocity anti-nodes (see Figure 6). In the vicinity of the velocity anti-node phase-shift is expected to vary continuously from $-\pi$ to $+\pi$ (see Figure 2 mode GD-A) (Baillot and Lespinasse (2014)). Thus the phase difference between velocity and intensity anti-nodes is not expected to remains null. Measurements are thus very sensitive to the position of the pressure transducers, which causes the phase-shifts of PT_{l0} with PT_{c0}, PT_{r0} or PT_{ref} to
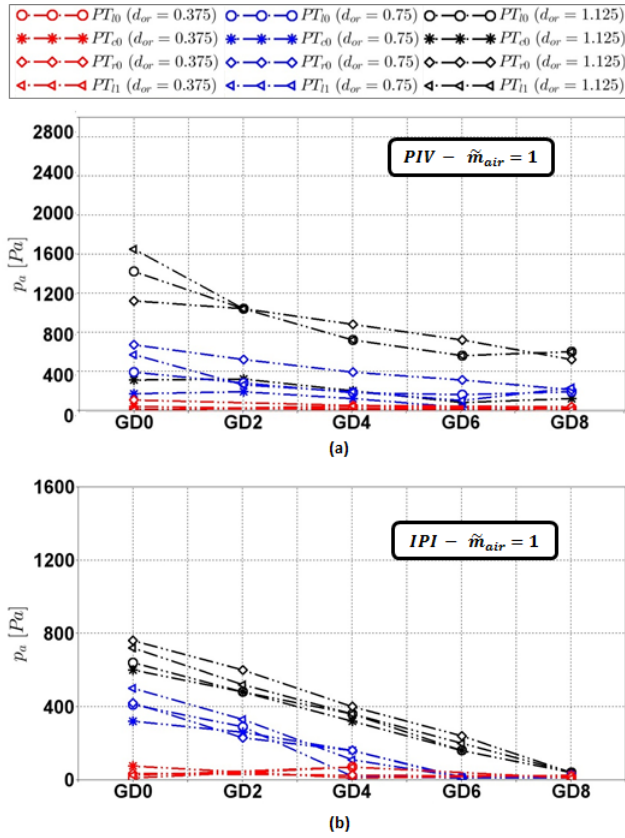
Figure 9. Acoustic response of the gas dome as a function of the dome size for the three connections diameters at: (a) PIV, $\tilde{m}_{air} = 1$ and (b) IPI, $\tilde{m}_{air} = 1$.

Figure 10. Experimental phase-shifts between the PT_{l0} signal and PT_{c0}, PT_{r0}, PT_{l1} and PT_{ref} signals as functions of the dome size, for $d_{or} = 0.75$ (left side) and $d_{or} = 1.125$ (rigth side) at: (a) IVI, (b) PIV and (c) IPI.

vary with the dome size for both $d_{or} = 0.75$ and $d_{or} = 1.125$ (see Figure 10(b)). The acoustic pressure fluctuations at any point in the dome decreases by increasing its size, which is in agreement with calculation of Figure 2.

The IPI configuration is centred in the cavity, thus, the three injectors are submitted to the maximum and in-phase acoustic solicitation, i.e. $\approx$12 kPa. This kind of solicitation facilitates the establishment of the GD-C mode (see Figure 2 mode GD-C). This is confirmed experimentally by in-phase (see Figure 10(c)) and same amplitude (see Figure 9) pressure signals in the dome. For $d_{or} = 0.75$ phase-shifts are independent from the dome size while for $d_{or} = 1.125$ they slightly change by increasing the dome size. This slight change is due to the fact that the mode shape changes in this case. Indeed, simulations indicate that, when dome size is increased, the eigenmode changes its mode shape (see Figure 2 mode GD-C). A good agreement between pressure amplitudes measured by PT_{l1}, PT_{l2} and PT_{l3} and predicted by simulations is shown in Figure 11. Simulations are made by considering the main cavity and gas dome simultaneously. Numerical curves are scaled by the maximum experimental value, indicated as A_i in the figure. The appearance of the nodal line is clearly visible at $GD8$. Contrary to what is
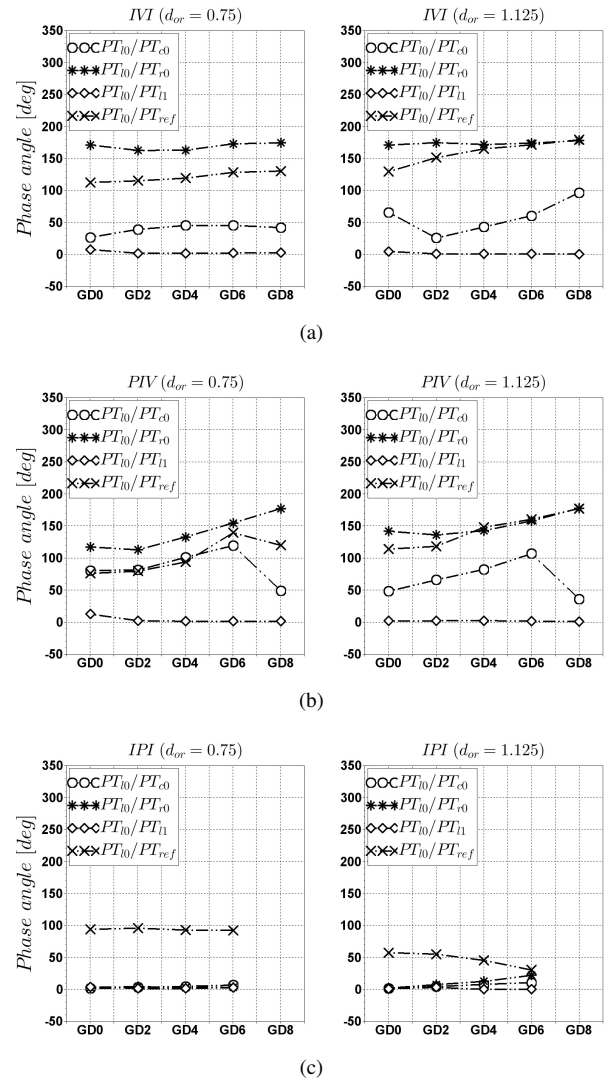
observed in the two other configurations, an increasing in the dome size at IPI does not induce a decrease of acoustic pressure fluctuation amplitudes in all points. Indeed, pressure amplitude measured with PT_{l3} at $GD8$ is higher than the one measured by PT_{l0} at $GD0$, due to the mode shape veering. Acoustic pressure amplitudes detected in the dome are always lower than 800 Pa, which corresponds to 6.7% of the acoustic pressure amplitude imposed in the main cavity at PAN. However, even if the cavity acoustic pressure amplitudes are maximum at IPI the response of the dome in this configuration is always lower than the two other cases. The fact that the maximum acoustic response in the dome does not correspond to the maximum acoustic pressure fluctuations in the cavity confirms that an acoustic coupling mechanism is established.
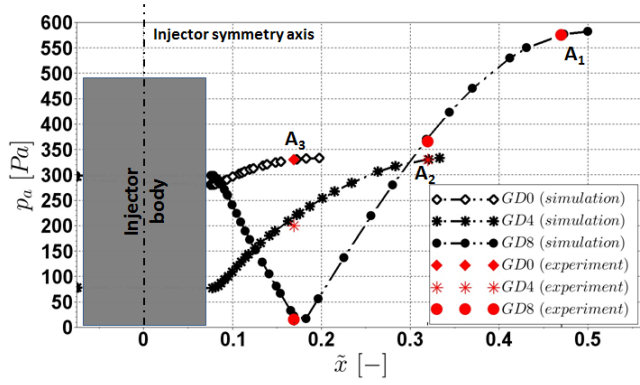
Figure 11. Numerical acoustic pressure amplitude, along the gas dome width compared to experimental measurements (each curve is scaled by the maximum value A_i, with $i \in (1, 3)$).

The acoustic response of the gas dome strongly depends on the considered parameters and the dependence on such parameters has a unique tendency. For all configurations, the acoustic coupling between the dome and the main cavity is discouraged by increasing the mass flow rate, the dome size and by decreasing the connection diameters. The only exception is represented by IPI. In this latter configuration acoustic pressure amplitudes measured in the dome decrease with the dome size until $GD6$; for a further increment of the dome size the acoustic pressure amplitude measured in GD increases. By changing the position of the dome with respect to the acoustic axis, different excitation conditions are imposed to the injection system and consequently different mode shapes are excited into the injection dome. Mode shapes observed experimentally are in agreement with the numerical simulations.

Acoustic response of the liquid dome

For the investigation of the acoustic response of the liquid dome a total of 60 test cases has been performed, combining:

- five dome sizes, named: $LD0$, $LD05$, $LD1$, $LD15$, and $LD2$, with $LD0$ representing the smallest dome volume and $LD2$ the biggest one;
- two injector connection lengths (scaled with the injector length): $L_j = 0.387$, $L_j = 0.548$;
- two injector connection diameters (scaled with the injector exit diameter): $d_j = 0.67$, $d_j = 1$;
- three spatial configurations of the injection system with respect to the acoustic axis (see Figure 6).

Figure 12 shows the amplitudes recorded by PT_l and PT_r (presented in the sketch of Figure 7) while Figure 13 shows the phase-shift between their signals. Both quantities are expressed as functions of the dome size, L_j and d_j for the three spatial configurations considered (IVI, PIV and IPI).

For the IVI configuration the LD acoustic pressure amplitudes are always lower than 1200 Pa (10% of the maximum acoustic pressure in the main cavity). Changing the junction diameter, length or the dome size does not seem to have an effect on the dome response. The acoustic pressure signals measured with PT_l and PT_r are out-of-phase. The phase-shift between transducers suggests an acoustic pressure spatial distribution similar to that of the LD-B mode shape (see Figure 4).

In the PIV configuration the response is more sensitive to the dome size and the acoustic pressure amplitudes decrease with the dome size. A peak is measured for $LD05$: it equals 2000 Pa for the shortest junction length and diminishes to 1200 Pa for the longest one. The phase-shift between the transducers is in between 40° and 120° which does not correspond to those of the simple eigenmodes calculated and presented in Figure 2.

For the IPI configuration and for $L_j = 0.387$ acoustic pressure amplitudes are the lowest and do not exceed 700 Pa. By increasing the junction length ($d_j = 0.67$), a stronger response of the liquid dome is obtained and two peaks of 1600 Pa and 1250 Pa are observed for $LD0$ and $LD1$. For $d_j = 1$ the two pressure transducers signals are perfectly in-phase with $L_j = 0.387$, indicating the possible onset of the mode LD-A (see Figure 4 mode GD-A), while with $L_j = 0.548$ the response is more complex. For $d_j = 0.67$ pressure transducers phase-shift decreases from 100° for $L_j = 0.387$ and 60° for $L_j = 0.548$ to 0°.

Results indicate that in some conditions the liquid dome can manifest acoustic pressure fluctuations of the same order of magnitude of the one observed in the gas dome. The general tendency is to discourage the acoustic response by increasing the dome size. However, results indicate that the LD acoustic response is more complex if compared with the one observed for the gas dome. A unique dependency of amplitude fluctuations on the parameters considered here is difficult to identify.

Conclusion

The acoustic interaction between a high-amplitude transverse acoustic field and an injection system has been investigated. A large parametric analysis has been performed and the response of the system has been tested in several configurations. The objective of this investigation was to observe how an injection system could respond to the acoustic pressure fluctuations coming from an instability established in a combustion chamber.
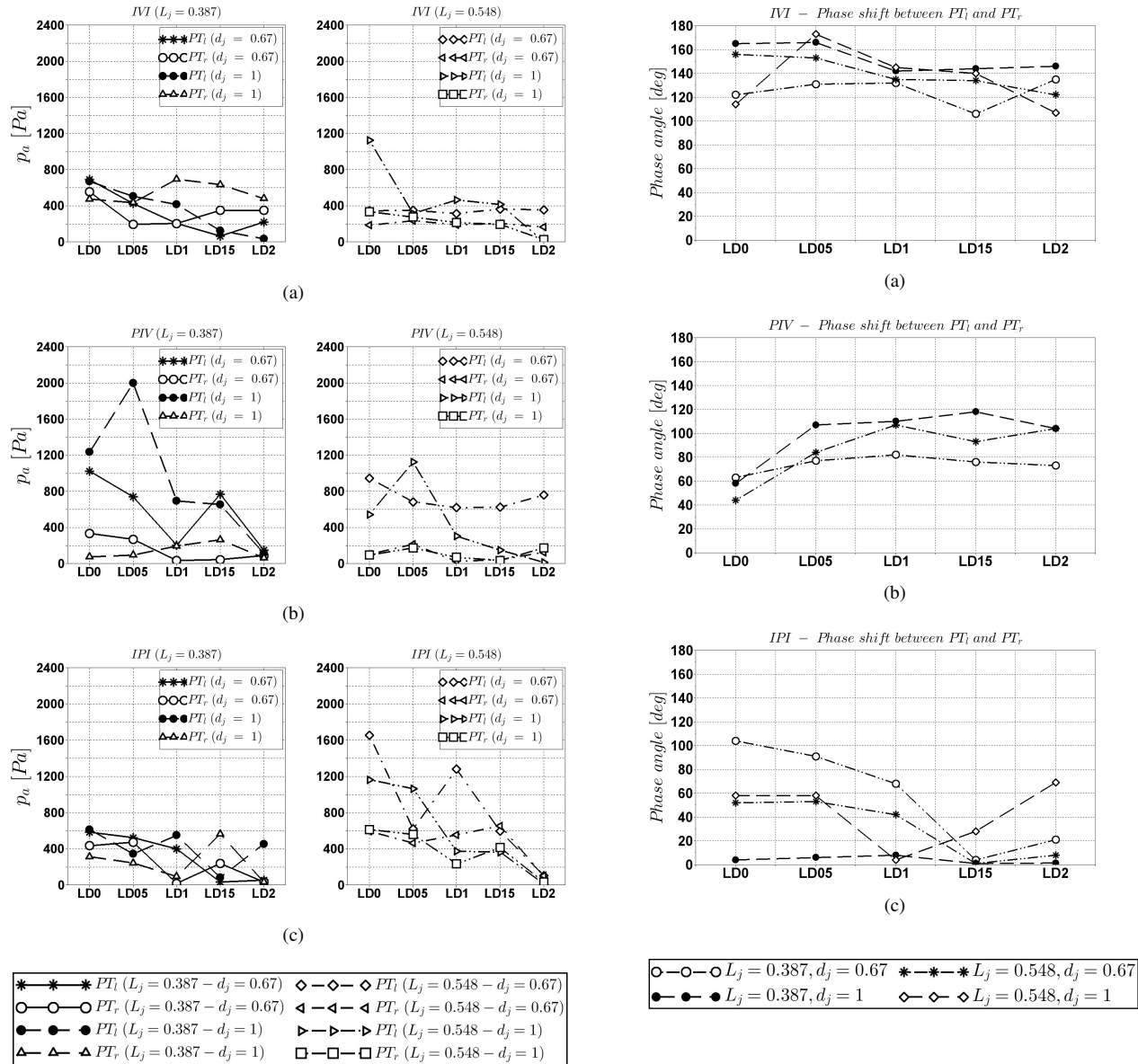
Figure 12. Acoustic response of the liquid dome as a function of the dome size for the three connection lengths at: (a) IVI, (b) PIV and (c) IPI.

Figure 13. Experimental phase-shift between the PT_l and PT_r signals as function of the dome size and L_j at: (a) IVI, (b) PIV and (c) IPI.

Two injection domes, one for the gas and one for the liquid, have been expressly designed in order to investigate the acoustic coupling at the forcing frequency of 1kHz. The two domes were used to feed three coaxial injectors similar to those used in liquid rocket engines applications.

By changing the position along the acoustic axis, different excitation conditions are imposed to the injection system and thus different mode shapes are excited into the injection domes. In most of the cases, eigenmode simulations allow identifying the mode shapes excited experimentally. But in some cases, the response of the domes, particularly the liquid dome, is more complex and direct identification is not possible.

The response of the injection system is strongly affected by the acoustic boundary conditions at injector outlets and by all the geometrical parameters considered here. In all the configurations, the acoustic coupling between the gas dome and the main cavity is discouraged by increasing the mass flow rate, the dome size and by decreasing the diameter of the connections between the injectors and the gas dome. The only exception is represented by the IPI configuration, in which an excessive increase of the dome size causes an increase of the acoustic response. For the IVI configuration the boundary conditions imposed at the injectors exit plane, in terms of acoustic pressure amplitudes in the main cavity, are lower than those corresponding to PIV and IPI configurations. However, the gas dome manifests the strongest acoustic response for this configuration.

This confirms the establishment of an acoustic coupling mechanism between the main cavity and the dome.

For what concerns the liquid dome response, the general tendency is to discourage the acoustic coupling by increasing its size. The response of LD does not seem to be strongly sensitive to the parameters studied here for the IVI configuration. However, the liquid dome manifests a strong acoustic response in some conditions for PIV and IPI configurations.

The main conclusion is that both liquid and gas domes show a strong response to the transverse acoustic field established in the main cavity. The maximum of acoustic pressure fluctuation amplitudes attains 17 % of the amplitudes of the acoustic pressure forced in the main cavity. In an actual propulsion system, such a high level of fluctuations in the injection dome could induce strong mass flow rate fluctuations. In fact, mass flow rate fluctuation can give a significant contribution to the acoustic fluctuations amplification in the combustion chamber.

Moreover, the maximum response of the domes is not observed in the configuration where the injection system is submitted to the highest acoustic pressure fluctuations of the cavity (IPI configuration), but mostly where the phase-shift conditions can excite a particular dome eigenmode, as in the IVI configuration for the gas dome.

Acknowledgements

References

Yang V. and Anderson W. (1995) *Liquid Rocket Engine Combustion Instability*, Pennsylvania State University.

Harrje, D. J. and Reardon, F. H. (eds.), 1972, *Liquid Propellant Rocket Combustion Instability*, NASA SP-194.

Oefelien J. C. and Yang V.(1993) *Comprehensive Review of Liquid-Propellant Combustion Instabilities in F-1 engines*, Journal of Propulsion and Power, Vol. 9, No. 5, pp. 657-677.

Fisher S. C., Dodd F.E. and Jensen R.J (1995) *Scaling techniques for Liquid Rocket Combustion Stability Testing*, Vol. 169, AIAA, Washington DC, pp. 545-564.

Hutt J. J. and Rocker M. (1995) *High-Frequency Injection-Coupled Combustion Instability*, Vol. 169, AIAA, Washington DC, pp. 345-555.

Baillot F., Blaisot J.B., Boisdron G. and Dumouchel C. (2015) *Behaviour of an air-assisted jet submitted to a transverse high-frequency acoustic field*, Journal of Fluid Mechanics, vol. 640, pp. 305-342.

Ficuciello A., Blaisot J.B., Baillot F., Richard C. and Théron M. (2015) *Response of coaxial air-assisted liquid jets in an acoustic field: atomization and droplets clustering*, 13th Triennial International Conference on Liquid Atomization and Spray Systems, Tainan, Taiwan.

Baillot F. and Lespinasse F. (2014) *Response of a laminar premixed V-flame to a high-frequency transverse acoustic field*, Combustion and Flame, vol. 161, pp. 12471267.